Using Field Simulations to Understand Susceptibility Related Phase Contrast in High Field Gradient Echo Images

A. Schäfer[1], P. A. Gowland[1], and R. Bowtell[1]

[1]Sir Peter Mansfield Magnetic Resonance Center, School of Physics and Astronomy, University of Nottingham, Nottingham, United Kingdom

Introduction

The small differences in magnetic susceptibility between tissues generate local magnetic field perturbation leading to variation of the NMR frequency. The resulting phase changes in gradient echo images form the basis of susceptibility weighted imaging (1,2), which has been exploited in generating enhanced venous contrast (2). More recently phase images obtained at 7 T have been shown to provide an enhanced grey to white matter contrast compared with modulus data and to allow the delineation of cortical sub-structure (3). The nature of this phase contrast has not however been explored in detail and in particular important questions remain about its quantitative nature and level of localization. Here, we use a recently developed method for simulating the field perturbations produced by a general distribution of magnetic susceptibility (4,5) to explore the relationship between the form of the susceptibility distribution and phase image contrast. The results of these simulations have been compared with experimental data acquired at 7 T from human subjects to provide new insight into the relationship between phase and anatomy.

Methods

Theory: The field perturbation due to a susceptibility distribution, $\chi(\mathbf{r})$ exposed to a magnetic field, B_0, applied in the z-direction was evaluated by inverse 3D Fourier transformation (FT) of $B_0 X(\mathbf{k})(1/3-\cos^2\beta)$, where $X(\mathbf{k})$ is the 3DFT of $\chi(\mathbf{r})$ and β is the angle between $\mathbf{k}$ and the k_z-axis (4,5). This approach has the advantage of naturally including the effect of the sphere of Lorentz so that multiplication of the calculated field offset by the magnetogyric ratio γ, directly yields the NMR frequency offset (5). Field changes due to object rotation may also be simply evaluated (5).

Simulation: Simulations were carried out on susceptibility distributions based on: (i) the whole head of the HUGO body model (Medical VR Studio, Lörrach) with 1 mm isotropic resolution; (ii) a simple model of the substantia nigra (SN) and red nuclei (RN). Tissue susceptibility values were taken from the literature [Grey Matter (GM): -8.97; White Matter (WM): -8.80; Bone: -8.4; CSF: -9.04; Fat: -7.79; Air: 0 all in ppm] (6). A susceptibility difference of 1 ppm between the SN/RN and surrounding tissue was arbitrarily set. Simulations based on 3D matrix sizes of 256^3 or 512^2 x 150 were carried out.

Experiment: Experimental data were acquired on a 7T Philips Achieva scanner incorporating a 16 channel helmet receiver coil using a flow-compensated, 3D spoiled gradient echo sequence with 0.4 mm isotropic resolution on a 480 x 480 x 100 matrix, TE/TR = 20/45 ms and $\alpha = 15^o$. Three echoes were acquired per excitation giving a total image acquisition time of 12 minutes.

Analysis: Both the simulated and experimental data were high-pass filtered to remove phase variations occurring on a large length scale (1,2). This was accomplished by subtraction of a 2D polynomial fit to the phase maps or by dividing the original complex data by a low-pass filtered version, formed via 2D Gaussian Fourier filtering. The effect of using filter widths of 4, 8 and 16 mm FWHM was explored.

Results and Discussion

Figure 1 shows experimental (Figs.1a-c) and simulated (Figs. 1d-f) data from similar superior axial slices in the brain with the magnetic field oriented in the superior-inferior direction. After removal of large length-scale effects, both the measured (Fig. 1c) and simulated data (Fig. 1f) still show significant local variation of the field/phase, with sharp boundaries between GM and WM regions reflecting the small differences in magnetic susceptibility between these tissues. Analysis of the results of simulations with varying field orientation with respect to the object shows that GM/WM boundaries are sharpest in slices oriented perpendicular to the field. The frequency difference between GM and WM in the experimental data depends on the filter size taking values of 1.75 ± 0.9Hz (0.006 ± 0.003 ppm), 2.9 ± 0.9Hz (0.097 ± 0.003 ppm) and 3 ± 1Hz (0.010 ± 0.004 ppm) for the filters with 4, 8 and 16 mm FWHM respectively. A similar increase in the absolute value of the GM/WM frequency difference with filter width is found in the simulated data, which yields values of 0.015 ± 0.005 , 0.026 ± 0.007 and 0.027 ± 0.01 ppm, respectively for filters with 4, 8 and 16 mm FWHM. Comparison of experimental and simulated values of the frequency difference indicates that the GM/WM susceptibility difference is over-estimated by a factor of approximately 3 in the literature and of the wrong sign – the experimental data shows that GM has a more positive susceptibility than WM, but the opposite holds in the literature values (6). The GM/WM frequency difference in the simulated data is less than the value of -0.057 ppm that would be predicted by simply equating to the value of $\Delta\chi/3$ (3), where $\Delta\chi$ is the GM/WM susceptibility difference.

Figure 2 shows experimental data acquired at the level of the substantia nigra (Figs 2a & b) along with simulated data produced using a simple model (Figs. 2e & f) formed by tracing the shapes of the substantia nigra and red nuclei in the magnitude images (Fig. 2a). The measured and simulated data (Figs. 2b and 2f) show quite similar patterns of field variation. Both manifest a dark ring surrounding the RN and a positive to negative field change on moving across the SN in a medial to lateral sense. This change is more significant in the experimental data probably reflecting a variation in susceptibility across the SN. Even after spatial filtering the simulated field map in a slice positioned approximately 4 mm above the simple model of the SN and RN (Figure 2g) shows a structured field variation (Figure 2h). This is also evident in the experimental data (Figs 2c & d), indicating that a "shadow" of a structure may be projected into adjacent slices in phase images. To investigate this phenomenon further we also simulated field shifts due to a simple sphere (Figures 2i & k). A dark ring around the sphere (Fig. 2j) and "shadow" in a slice above the sphere (l) are also evident in this case. The ring appearing in phase images of the RN has previously been related to anatomical structure, but its presence in the data from a simulated sphere indicates that this is not the case.

Conclusion

Forward calculations of the field perturbation due to the susceptibility distribution in the human head provide some insight into phase contrast obtained in GE images. Importantly they show that features of phase images may not correspond directly to anatomical features. In the cortex, phase approximately reflects the local value of susceptibility. In more localized structures such as the substantia nigra and red nuclei the behavior is more complex and phase changes occur remotely.

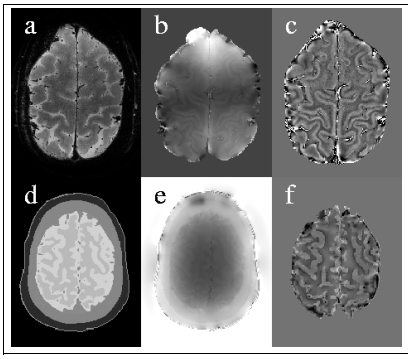

Figure 1: Experimental modulus (a), unwrapped phase data (b) and spatially filtered phase data (c); HUGO model (d), calculated field (e) and spatially filtered field data (f). The field has been negated in these maps to allow better comparison of experimental and simulated data.

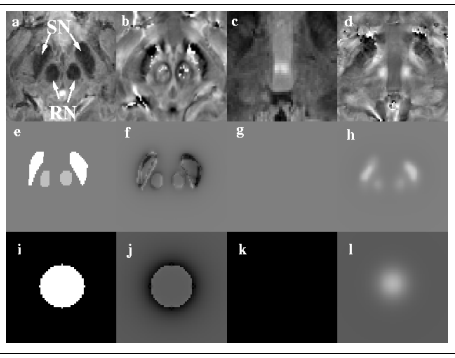

Figure 2: Experimental modulus (a,c) and phase data (unwrapped and spatially filtered; b,d). Simple model (e,g) and resulting phase data, at the level of (f) and 4 mm above, the SN and RN (h). The middle slice of a sphere (i) and related field-shift (j), similar data from a second slice above the sphere (k,l).

References

[1] EM Haacke *et al* Magn. Res. Med. 52:612-618, 2004. **[2]** EM Haacke *et al* Magn. Res. Imag. 23:1-25, 2005. **[3]** J Duyn *et al* PNAS 104 :11796-11801, 2007 **[4]** R Salomir *et al*, Conc. MR 19B: 26-34, 2003. **[5]** JP Marques, R Bowtell, Conc. MR 25B: 65-78, 2005. **[6]** CM Collins *et al* Mag. Res. Imag. 20:413-424, 2002.